Materials Research Letters

ISSN: (Print) 2166-3831 (Online) Journal homepage: http://www.tandfonline.com/loi/tmrl20

Multicomponent equiatomic rare earth oxides

Ruzica Djenadic, Abhishek Sarkar, Oliver Clemens, Christoph Loho, Miriam Botros, Venkata S. K. Chakravadhanula, Christian Kübel, Subramshu S. Bhattacharya, Ashutosh S. Gandhi & Horst Hahn

To cite this article: Ruzica Djenadic, Abhishek Sarkar, Oliver Clemens, Christoph Loho, Miriam Botros, Venkata S. K. Chakravadhanula, Christian Kübel, Subramshu S. Bhattacharya, Ashutosh S. Gandhi & Horst Hahn (2017) Multicomponent equiatomic rare earth oxides, Materials Research Letters, 5:2, 102-109, DOI: 10.1080/21663831.2016.1220433

To link to this article: https://doi.org/10.1080/21663831.2016.1220433

MATER. RES. LETT., 2017
VOL. 5, NO. 2, 102–109
http://dx.doi.org/10.1080/21663831.2016.1220433

MATERIALS RESEARCH LETTERS
Taylor & Francis
Taylor & Francis Group

ORIGINAL REPORT

OPEN ACCESS

Multicomponent equiatomic rare earth oxides

Ruzica Djenadic[a,b], Abhishek Sarkar[c,d], Oliver Clemens[b], Christoph Loho[b], Miriam Botros[b], Venkata S. K. Chakravadhanula[a,c], Christian Kübel[c,e], Subramshu S. Bhattacharya[d], Ashutosh S. Gandhi[f] and Horst Hahn[a,b,c]

[a]Helmholtz Institute Ulm—Electrochemical Energy Storage, Ulm, Germany; [b]Joint Research Laboratory Nanomaterials—Technische Universität Darmstadt and Karlsruhe Institute of Technology, Darmstadt, Germany; [c]Institute of Nanotechnology, Karlsruhe Institute of Technology, Eggenstein-Leopoldshafen, Germany; [d]Indian Institute of Technology Madras, Chennai, India; [e]Karlsruhe Nano Micro Facility, Karlsruhe Institute of Technology, Eggenstein-Leopoldshafen, Germany; [f]Indian Institute of Technology Bombay, Mumbai, India

ABSTRACT

Multicomponent rare earth oxide (REO) nanocrystalline powders containing up to seven equiatomic rare earth elements were successfully synthesized in a single-phase CaF_2-type (*Fm*-3 *m*) structure. The addition of more than six elements resulted in the formation of a secondary phase. Annealing at 1000°C for 1 h led to the formation of a single-phase (*Ia*-3) even in the 7-component system. In the absence of cerium (Ce^{4+}), secondary phases were observed irrespective of the number of cations or the extent of thermal treatment indicating that cerium cations played a crucial role in stabilizing the multicomponent REOs into a phase pure structure.

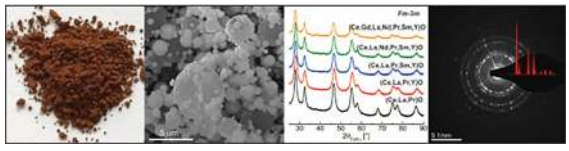

IMPACT STATEMENT

Multicomponent equiatomic rare earth oxides pioneer a new group of materials that crystallize into a single-phase structure with the dominant role of a single element instead of entropy.

ARTICLE HISTORY
Received 9 June 2016
Accepted 31 July 2016

KEYWORDS
Rare earth oxide; entropy; single phase; nanocrystalline

Introduction

The success in identifying novel materials with complete disorder, improved properties, lower costs, better environmental compatibility, etc., constitutes a major foundation for the development of new technologies and products. Recently, it was shown that a crystalline single-phase oxide containing five transition metal ions in equiatomic amounts ($Mg_{0.2}Co_{0.2}Ni_{0.2}Cu_{0.2}Zn_{0.2}O$) can be synthesized.[1] Consequently, the new material was named 'entropy-stabilized oxide' (ESO) due to the high configurational entropy possible in a multicomponent system. The possibility of synthesizing an oxide system comprising five elements in a single phase is surprising, especially when taking into account that some of the binary oxides of these elements possess different crystal structures in their pure form (e.g. hexagonal wurtzite-type ZnO, monoclinic CuO). The principal idea originates from the field of multicomponent metallic alloys, widely known as high-entropy alloys (HEAs), which are defined as solid solutions containing 'multiple principal elements (five or more) in equimolar or near-equimolar ratios'.[2] HEAs have a range of remarkable mechanical (strength, hardness, ductility, wear resistance), physical (magnetic, conductivity), and chemical (corrosion resistance) properties [3–5] as compared to the conventional alloys with one or two principal elements. In such metallic systems, the high configurational entropy thermodynamically stabilizes a single-phase solid solution through a reduction of the Gibbs free energy.[2] In analogy, to HEAs, Murty et al. [5] suggested that a similar mixing entropy effect in ceramics and polymers can be expected. Although

CONTACT Ruzica Djenadic djenadic@nano.tu-darmstadt.de Joint Research Laboratory Nanomaterials—Technische Universität Darmstadt and Karlsruhe Institute of Technology, Darmstadt 64287, Germany

Supplemental data for this article can be accessed here. http://dx.doi.org/10.1080/21663831.2016.1220433

research on high-entropy ceramics, carbide- and nitride-based, has already been tackled,[6–8] the synthesis of high-entropy oxide-based ceramic systems has not been reported until recently. Rost et al. [1] showed successfully that oxide systems can be entropy stabilized by synthesizing microcrystalline $Mg_{0.2}Co_{0.2}Ni_{0.2}Cu_{0.2}Zn_{0.2}O$, which exhibited a single-phase rock-salt-type structure. The full potential of ESO materials with rock salt or other possible crystallographic structures is yet to be discovered. The first study of the microcrystalline $Mg_{0.2}Co_{0.2}Ni_{0.2}Cu_{0.2}Zn_{0.2}O$ system [9] showed a 'colossal dielectric constant' of 2×10^5 at 440 K with bulk resistance of 30 MΩ being three orders of magnitude higher than the resistance of the mixture of any of the binary oxides. The authors believe that this system has the potential to be used as a large-*k* dielectric material. Doping (aliovalent or isovalent) of entropy-stabilized oxides could lead to even more exciting and diverse properties with possibly a wide range of applications.

In the present study, the possibility of synthesizing high-entropy rare earth oxides (REOs) containing five to seven rare earth (RE) elements as well as low and medium entropy oxides [5] comprising two to four RE elements in equiatomic amounts was explored. The nanocrystalline multicomponent REO powders were synthesized by employing nebulized spray pyrolysis (NSP) instead of solid-state reactions as done in previous publications.[1,9] This well-established method [10–15] allows for the direct synthesis of nanocrystalline powders in a short period of time (production rate of 1–2 g h^{-1} in a laboratory scale reactor) with a homogeneous distribution of the elements inside the crystal lattice. The crystal structure and the elemental compositions of as-synthesized and subsequently heat-treated REO powders are discussed and the phase stability upon heat treatments is addressed.

Experimental

Material synthesis

The following 'selection rules' were considered as a guide for the choice of the compositions: (*i*) cations should have similar ionic radii, (*ii*) at least one of the binary oxide systems should have a different crystal structure, and (*iii*) at least one binary oxide pair should not have complete miscibility at 0.5 mole fraction based on the oxide binary phase diagram. Table 1 provides the overview of crystal structures and space groups of single oxides of the RE elements [16–19] used in this study, corresponding cation oxidation state, coordination numbers, and ionic radii.[20]

Table 1. Crystal structures and space groups of single oxides [16–18], corresponding cation oxidation state, coordination numbers (CNs), and ionic radii (r_c) [20].

Oxide	Crystal system	Space group	Oxidation	CN	r_c (nm)
Ce_2O_3	Trigonal	*P*-3*m*1	3+	VII	1.07
CeO_2	Cubic (fluorite)	*Fm*-3*m*	4+	VIII	0.97
Gd_2O_3	Cubic	*Ia*-3	3+	VI	0.938
La_2O_3	Trigonal	*P*-3*m*1	3+	VII	1.1
Nd_2O_3	Trigonal	*P*-3*m*1	3+	VII	1.048[a]
Pr_2O_3	Trigonal	*P*-3*m*1	3+	VII	1.058[a]
PrO_2	Cubic	*Fm*-3*m*	4+	VIII	0.96
Sm_2O_3	Monoclinic	*C*2/*m*	3+	VI and VII	0.958 and 1.02
Y_2O_3	Cubic (bixbyite)	*Ia*-3	3+	VI	0.9

[a]Values deduced from ionic radii for VI and VIII coordination [20].

The REO nanopowders containing up to seven RE elements were synthesized using NSP. The experimental set-up is illustrated elsewhere, see [10,21]. The nitrate salts of Ce, Gd, La, Nd, Pr, Sm, and Y($Ce(NO_3)_3{\cdot}6H_2O$, ABCR, 99.9%; $Gd(NO_3)_3{\cdot}6H_2O$, Sigma-Aldrich, 99.9%; $La(NO_3)_3{\cdot}6H_2O$, Sigma-Aldrich, 99.9%; $Nd(NO_3)_3{\cdot}6H_2O$, Sigma-Aldrich, 99.9%; $Pr(NO_3)_3{\cdot}6H_2O$, ABCR, 99.9%; $Sm(NO_3)_3{\cdot}6H_2O$, ABCR, and 99.9%; $Y(NO_3)_3{\cdot}6H_2O$, Sigma-Aldrich, 99.9%) were used as precursors. A water-based solution containing appropriate equiatomic cation combinations (concentration of 0.1 mol L^{-1}) was continuously delivered ($\sim$120 ml h^{-1}) into the piezo-driven nebulizer. The generated mist containing fine droplets of the precursor solution was transported by flowing oxygen (5 standard l min^{-1}) into the hot-wall reactor. The nanoparticles, synthesized at 1150°C and a pressure of 900 mbar, were collected using a filter-based collector. The REO samples will be for the sake of simplicity labelled not according to their stoichiometric formulae, but according to the elements present, e.g. oxide system containing five RE elements will be labelled as (Ce,La,Pr,Sm,Y)O and further in the text, it will be addressed as 5-component REO system, etc. For easier comparison, RE elements are listed alphabetically, instead of based on their atomic number.

In order to get an insight into the phase formation and the phase stability of multicomponent REOs, several thermal treatment experiments were conducted. The first set of experiments was conducted to study formation of phases. In these experiments, 5- and 6-component powders with and without Ce, (Ce,La,Pr,Sm,Y)O, (Ce,Gd,La,Pr,Sm,Y)O, (Gd,La,Nd,Pr,Sm,Y)O, were annealed in air at 1000°C for 1 h with cooling/heating rates of 10°C·min^{-1}. The second set of experiments was performed to study the effect of entropy on the phase stabilization. Therefore, the 5-component powder, (Ce,La,Pr,Sm,Y)O, was heat treated in air at two different temperatures for different times and air quenched from the calcination temperature to room temperature. The following experiments were performed: (*i*)

calcination of the as-synthesized powder at 750°C for 1 h, (*ii*) calcination of the as-synthesized powder at 750°C for 2.5 h, and (*iii*) additional calcination at 1000°C for 1 h of the already calcined powder (750°C for 1 h).

Characterization

Room temperature X-ray diffraction (XRD) patterns of the as-synthesized powders were recorded using a Bruker D8 diffractometer with Bragg–Brentano geometry equipped with an X-ray tube with a Cu anode and a Ni filter. A LYNEXE detector and a fixed divergence slit (0.3°) were used. A step size of 0.02° and a collection time of 4 s at 30 kV and 40 mA over the 2θ angular range between 10° and 90° were used. Rietveld analysis (TOPAS 5, Bruker [22]) of the XRD patterns was used to determine the structure and phase composition of the as-synthesized and thermally treated powders. The instrumental intensity distribution for the XRD data was determined empirically from a fundamental parameter set, using a reference scan of LaB_6 (NIST 660a), and the microstructural parameters were refined (using two Voigt functions) to adjust the peak shapes. Thermal displacement parameters were constrained to be the same for all atoms of all phases to avoid quantification problems and to account for further effects such as absorption or surface roughness.

The microstructure of the powders was studied using a high-resolution scanning electron microscope, SEM (Philips XL30 FEG) and an aberration- (image) corrected FEI Titan 80–300 transmission electron microscope, TEM (FEI, Eindhoven, the Netherlands) equipped with a Gatan US4000 slow scan CCD camera (Gatan Inc., Pleasanton, CA). The particle size distribution (PSD) was determined from SEM images by measuring the size of approximately 500 particles using ImageJ 1.50a [23] and fitting the data by log-normal distribution function.

The elemental composition was determined using energy-dispersive spectroscopy (EDS) on a scanning electron microscope, SEM (ZEISS Gemini Leo 1530) equipped with INCA EDS X-ray spectrometer.

XPS analysis using PHI 5000 spectrometer and a monochromatic Al Kα (1486.6 eV) excitation source was used for determining oxidation states of Ce and Pr in the as-synthesized samples as they can have multiple stable oxidation states (3+ and 4+). Ce-oxide (CeO_2) and Pr-oxide (PrO_x) powders, synthesized by the same method as REO powders, were used as references. The photoelectron spectra were taken with 200 µm spot size at pass energy of 23.5 eV with energy steps of 0.1 eV. In order to compensate charging of the investigated oxides, a charge neutralizer with low-energy electrons is employed.

Results and discussion

Microstructure and element composition

The as-synthesized REO powders have a brown colour with apparent tint which decreases as the number of RE elements increases (Figure 1(a)). The morphology of the powders studied by SEM (Figure 1(b)) shows spherical agglomerates containing fine nanoparticles arranged in the form of hollow spheres with broad size distribution and a mean particle/agglomerate size of 560 nm. The EDS analysis (Table 2) confirms that nanocrystalline powders contain RE cations in equiatomic amounts

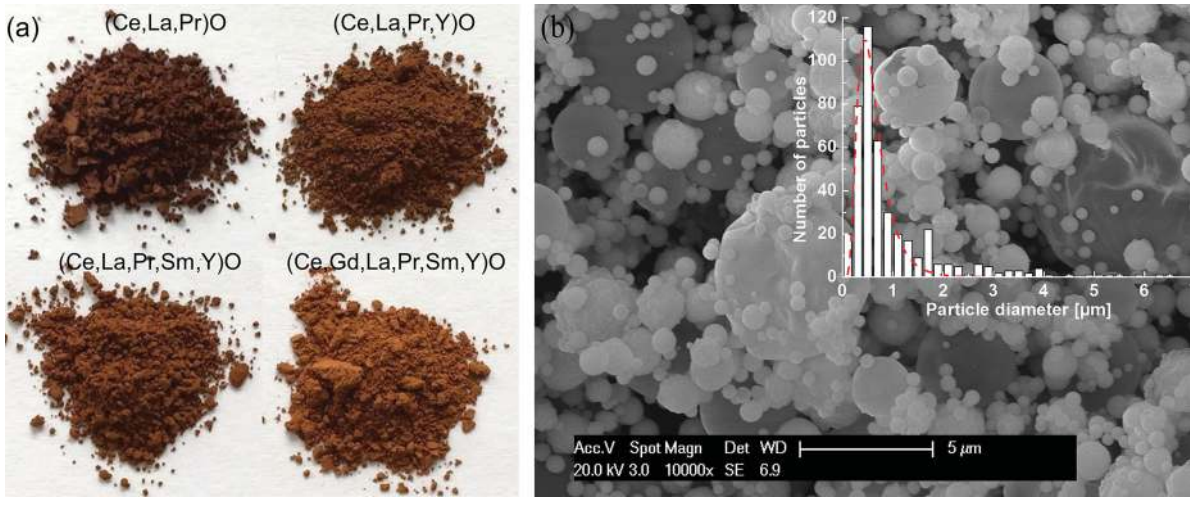

Figure 1. (a) Digital camera photographs of as-synthesized powders showing the change of powder colour from dark brown to light brown with increase in the number of RE elements and (b) SEM image with PSD of as-synthesized (Ce,La,Pr,Sm,Y)O powder as a representative of typical morphology of REO powders synthesized by the NSP method.

Table 2. Elemental composition (at. %) of selected REO powders obtained by analysis of EDS spectra.

Sample	Ce	Gd	La	Nd	Pr	Sm	Y
(Ce,La,Pr)O	12.3	–	12.9	–	12.5	–	–
(Ce,La,Pr,Y)O	8.6	–	8.4	–	8.6	–	8.7
(Ce,La,Pr,Sm)O	8.4	–	8.4	–	8.9	8.4	–
(Ce,La,Pr,Sm,Y)O	7.5	–	8.0	–	7.8	7.5	7.5
(Ce,La,Nd,Pr,Sm,Y)O	6.6	–	6.7	6.5	7.0	6.6	6.1
(Ce,Gd,La,Nd,Pr,Sm,Y)O	5.0	5.1	5.1	5.1	5.5	5.1	5.3

as desired and expected for powders synthesized by NSP.[10,12,24]

Selected REO powders were characterized using XPS in order to determine the oxidation state(s) of Ce and Pr (Figure 2). The XPS 3*d* spectra of Ce in CeO_2, (Ce,Pr,Sm)O, and (Ce,La,Pr,Sm,Y)O powders (Figure 2(a)) are very similar. The multiplet splitting containing six peaks can be identified in all three studied powders leading to the conclusion that Ce is present in 4+ oxidation state.[25] This is not surprising as it is known that Ce can be easily oxidized.[26] It can be assumed that the oxidation state of Ce (Ce^{4+}) in other synthesized REO powders is the same as the powders are synthesized under similar conditions (see experimental section).

The XPS 3*d* spectra of Pr in (Ce,Pr,Sm)O and (Ce,La,Pr,Sm,Y)O resemble the one obtained for Pr-oxide confirming that oxidation state of Pr is the same in all powders. Comparing the XPS data for Pr-oxide obtained in this work (Figure 2(b)) to the one reported in the literature,[27,28] the spectra indicate the presence of Pr^{4+} rather than Pr^{3+}, but mixed oxidation state [29] cannot be excluded. At present, based on XRD data (see SI, Figure S2b and S2c), it can only be assumed that Pr is most probably present in mixed oxidation state (Pr^{4+} and Pr^{3+}). To confirm the mixed valence state of Pr, more detailed analysis, especially X-ray absorption near edge structure (XANES) analysis, is needed.

Structure and phase composition

Figure 3 displays the XRD patterns of as-synthesized REO systems with Ce (Figure 3(a)) and without Ce (Figure 3(b)). Rietveld analysis of the XRD patterns reveals that the crystallite size for all as-synthesized powders is below 10 nm (Table 3). The analysis of the XRD patterns containing Ce (Figure 3(a)) indicates that systems with three to six elements crystallize in a single-phase CaF_2 type (*Fm*-3 *m*) structure, which is a structure with higher symmetry than any of the binary trivalent REOs (see Table 1). In contrast, in the absence

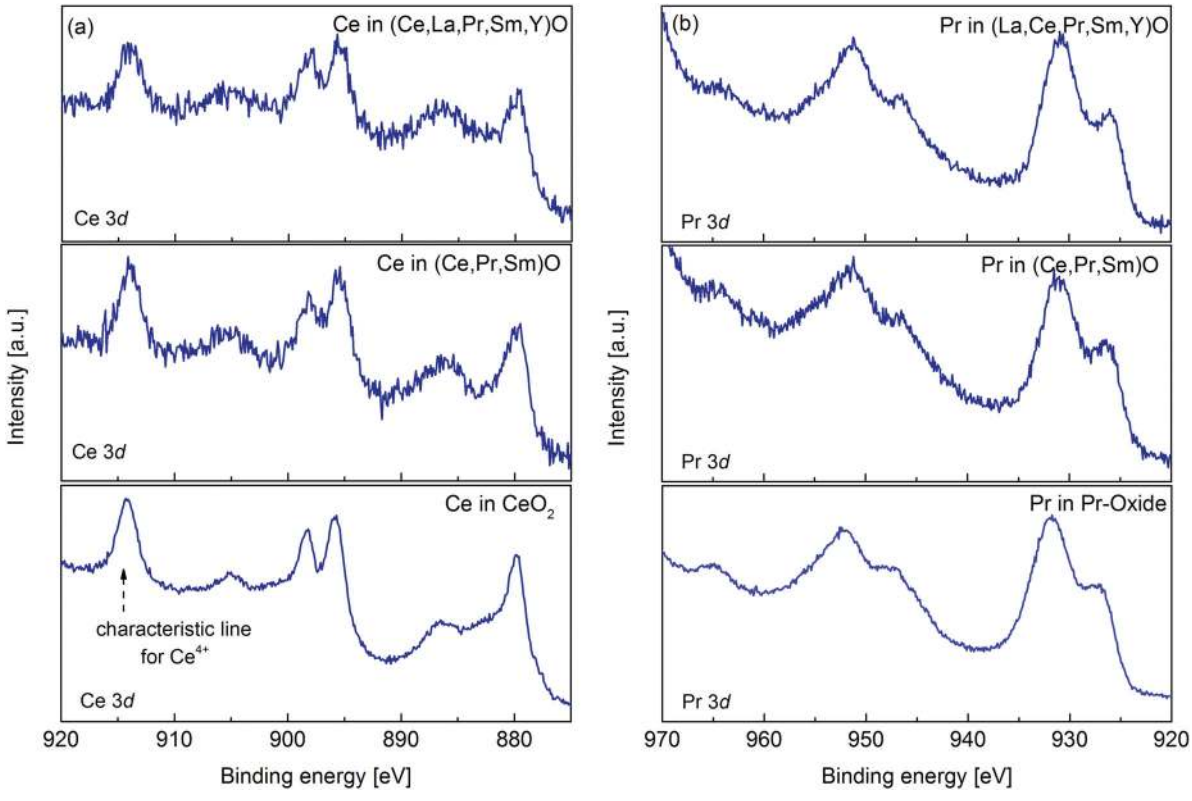

Figure 2. XPS 3*d* spectra of (a) cerium in CeO_2, (Ce,Pr,Sm)O, and (Ce,La,Pr,Sm,Y)O and (b) praseodymium in Pr-oxide, (Ce,Pr,Sm)O, and (Ce,La,Pr,Sm,Y)O.

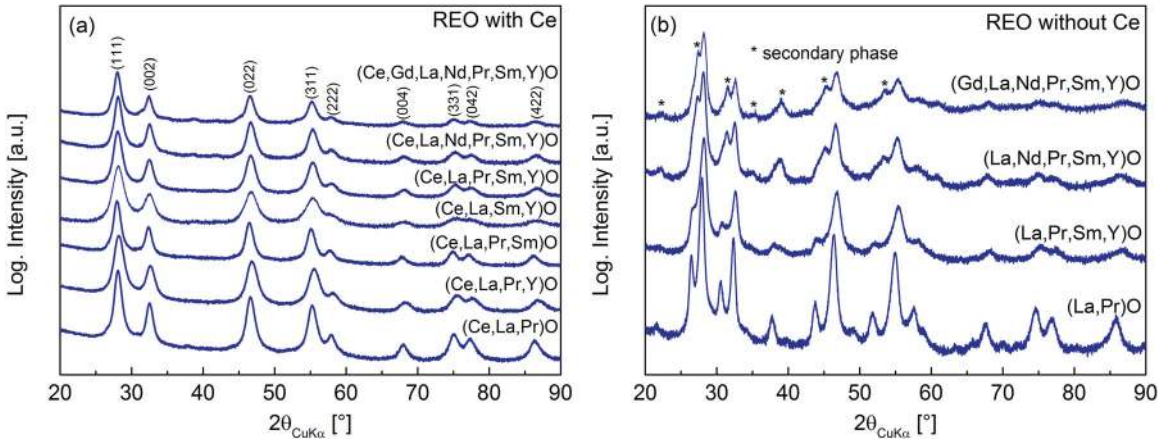

Figure 3. (a) XRD patterns of as-synthesized REO powders containing Ce (The indexed planes belong to the main phase, *Fm*-3 *m*) and (b) XRD patterns of as-synthesized REO powders without Ce (The formulae do not reflect powder stoichiometry—see experimental section.).

Table 3. Summary of results obtained by Rietveld refinement of as-synthesized and calcined REO powders (RE_2O_{3+y}, RE—equimolar amounts of RE elements) containing Ce: space group of main phase, fraction of main phase (*f*), lattice parameter (*a*), and crystallite size (*D*).

Sample, RE_2O_{3+y}	Space group	*f* (wt.%)	*a* (Å)	*D* (nm)
As-synthesized powders				
(Ce,La,Pr)O	*Fm*-3*m*	100	5.5203(2)	10.5(2)
(Ce,La,Pr,Y)O	*Fm*-3*m*	100	5.4962(3)	6.8(2)
(Ce,La,Pr,Sm)O	*Fm*-3*m*	100	5.5276(3)	7.8(2)
(Ce,La,Sm,Y)O	*Fm*-3*m*	100	5.5169(7)	8.4(4)
(Ce,La,Pr,Sm,Y)O	*Fm*-3*m*	100	5.5071(4)	7.5(2)
(Ce,La,Nd,Pr,Sm,Y)O	*Fm*-3*m*	100	5.4998(1)	–[a]
(Ce,Gd,La,Nd,Pr,Sm,Y)O	*Fm*-3*m*	97.1(1)	5.5168(4)	–[a]
Thermally treated powders without quenching, 1000°C/1h				
(Ce,La,Nd,Pr,Sm,Y)O	*Ia*-3	100	10.9625(2)	31(1)
(Ce,Gd,La,Nd,Pr,Sm,Y)O	*Ia*-3	100	10.9319(3)	34(2)
Thermally treated powders with quenching				
(Ce,La,Pr,Sm,Y)O;750°C/1h	*Fm*-3*m*	100	5.4869(2)	10.3(2)
(Ce,La,Pr,Sm,Y)O;750°C/2.5h	*Fm*-3*m*	100	5.4884(3)	8.5(2)
(Ce,La,Pr,Sm,Y)O;1000°C/1h	*Ia*-3	99.0(5)	10.9557(2)	28.8(7)

[a]Main contribution to peak broadening arises from strain.

of Ce, the studied systems do not crystallize as a single phase (Figure 3(b)), indicating the vital importance of this specific element. According to Pauling's rule of parsimony,[30] crystallization within a single simple structure is usually favoured over complex structures whenever the cations are similar regarding their size and oxidation state and they tend to be randomly distributed. In some HEA systems, it was observed that single-phase formation is governed by the binary pairs of elements in which other elements dissolve [5,31] and the alloy adopts the structure of the binary system with the highest ordering energy. Therefore, the distinct structural impact of Ce in comparison to the other elements present is further studied. Rietveld analysis of Ce-oxide synthesized by NSP reveals that under the same conditions used for REO synthesis (see experimental section), Ce-oxide crystallizes in a fluorite-type structure (*Fm*-3 *m*) (see SI, Figure S1a) and have composition of CeO_2 (i.e. Ce is tetravalent) which agrees with the literature,[26] and it was confirmed by XPS (see Figure 2(a)).

Based on these findings, in the REOs studied here, CeO_2 can be considered as the parent structure into which the other cations 'dissolve', by randomly substituting Ce^{4+} ions. Apart from Ce-oxide, the pure Pr-oxide also crystallized in a fluorite-type structure with composition $PrO_{\sim 1.83}$, i.e. Pr_6O_{11} when synthesized under similar conditions as all REOs (see corresponding XRD pattern in SI, Figure S1b and S1c). However, although the structures of the binary oxides of Ce and Pr are rather similar, those elements behave quite differently regarding their oxidation states, especially when brought into different chemical environments with different additional chemical elements. Whereas Ce can be only reduced to an oxidation state lower than 4+ by using highly reductive conditions,[26,32] Pr^{3+} can be easily stabilized by adjusting the size of the cation site by changing the chemical composition (i.e. reacting it with other metal oxides), even at oxidizing conditions in air atmosphere.[33] Therefore, the Pr oxidation state can be highly flexible depending on the chemical environment and complex to determine, whereas Ce is fixed to its tetravalent state. These findings imply that the composition of the as-prepared samples must follow a formula RE_2O_{3+y} whenever Ce is present in the mixture, and that the mechanism of phase stabilization can be considered to be different for the REO systems compared to the entropy-stabilized transition metal oxides reported previously.[1]

In the 7-component system containing Ce, (Ce,Gd,La,Nd,Pr,Sm,Y)O (Figure 3(a)), the formation of a minor secondary phase (La_2O_3, *Ia*-3, below 3 wt%, Table 3) is observed. The formation of secondary phases can

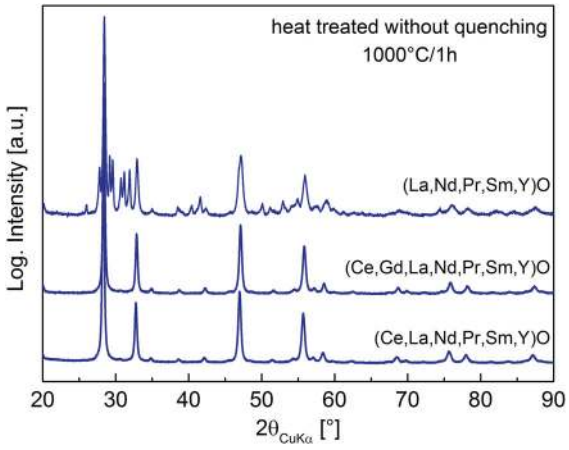

Figure 4. XRD patterns of heat-treated REOs at 1000°C for 1 h in air (heating/cooling rate 10°C min^{-1}).

be caused by so-called 'sluggish' diffusion [5,34] due to increased number of elements present in the system, which are competing for the same position in the lattice, rather than their insolubility in the fluorite structure. Therefore, it can be expected that even REO systems with more than six elements might be obtained as a single-phase system under conditions which would provide sufficient time for the diffusion of all elements to their desired lattice sites. This could, for example, be achieved *in situ* by increasing the residence time of particles inside of the hot-wall reactor, or *ex situ* by annealing which was conducted in this study. The XRD pattern of the 7-component system with Ce that is annealed at 1000°C for 1 h (heating/cooling rate 10°C·min^{-1}) (Figure 4) shows single-phase fluorite related, confirming that even the 7-component system containing Ce can crystallize into a single-phase structure if the system is supplied with sufficient energy and/or time for atom diffusion to desired sites in the crystal lattice. This single-phase structure is identified as *Ia*-3 (a lower symmetry derivative structure of *Fm*-3 *m*, see SI, Figure S3).

In contrast to the Ce-containing systems, heat treatment of the system without Ce, (Gd,La,Nd,Pr,Sm,Y)O, did not result in homogenization and the formation of a single phase (Figure 4), confirming once again that Ce acts as a stabilizer of the structure of REOs.

The bright-field TEM image (Figure 5(a)) of the as-synthesized (Ce,La,Sm,Pr,Y)O powder shows the polycrystalline nature of the particles. The crystallinity of the particles is also confirmed by the selected area electron diffraction (SEAD) pattern (Figure 5(b)), which shows spotty ring patterns without any additional diffraction spots and rings of second phases agreeing with the XRD data. The measured interplanar spacings from the SAED pattern are in good agreement with the values obtained from Rietveld refinement of the corresponding XRD pattern (Figure 3(a)). The *d*-spacing and the corresponding planes identified from the diffraction rings are 0.317 nm (111), 0.276 nm (002), 0.195 nm (022), 0.166 nm (311), 0.160 nm (222), 0.137 nm (004), 0.126 nm (331), 0.123 nm (042), and 0.112 nm (422).

Phase stability upon heat treatment

The effect of entropy on single-phase stabilization of REOs was tested by heat treatment of the 5-component (Ce,La,Pr,Sm,Y)O system at two different temperatures and air quenching to room temperature. The resulting XRD patterns are shown in Figure 6. After calcination at 750°C for 1 and 2.5 h followed by air quenching, no phase separation is observed. This is further confirmed by Rietveld refinement (Table 3). However, additional

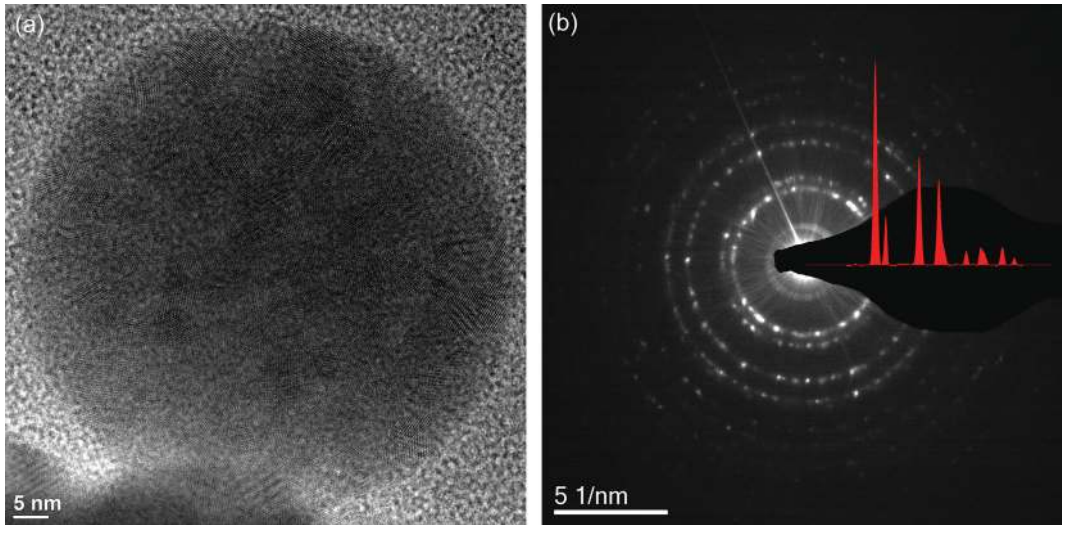

Figure 5. (a) Bright-field TEM micrograph and (b) corresponding SAED pattern of the as-synthesized (Ce,La,Pr,Sm,Y)O powder.

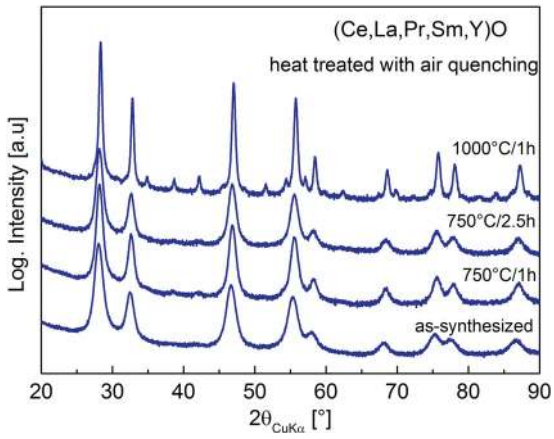

Figure 6. XRD patterns of heat-treated REOs at different temperatures followed by air quenching.

reflections are observed on heating the powder to 1000°C for 1 h. These reflections can be indexed using a body-centred cubic cell with a lattice parameter of $a_{bcc} \sim 2 \cdot a_{fcc}$ and is indicative of a lowering of symmetry from *Fm*-3 *m* to *Ia*-3 (see SI, Figures S3 and S4). The refined crystal structure and more details may be found in the SI) (Figures S3 and S4, Tables S1 and S2). Independent of the thermal treatment, the systems with 3–6 elements containing Ce (Figure 4) crystallize as single-phase compounds (Table 3) which is in contrast to entropy-dependent reversion from single phase to multiple phases at lower temperature reported by Rost et al. [1] indicating that entropy effect is not responsible for phase stabilization in REOs.

Conclusions

Multicomponent equiatomic REO systems containing up to seven RE elements were successfully synthesized using the NSP method. The strong differences in powder behaviour upon thermal treatment, in contrast with the previously reported entropy-stabilized transition metal oxides,[1] suggest that not only the entropy effect but also the type of elements present in the multicomponent system (i.e. element oxidation state), together with the influence of synthesis procedure (equilibrium, non-equilibrium), and crystallite size should be considered as factors that might play a role in the structure stabilization of multicomponent equiatomic oxides. In REO systems, cerium plays a crucial role in the phase stabilization. Not only experimental but also theoretical studies are needed to get a better insight into the underlying mechanism for single-phase formation in multicomponent REOs as well as other oxide systems that might emerge. Without any doubt, the results presented here and the recently published results [1,9] open a door into a new field of multicomponent equiatomic oxides with vast possibilities for research on their properties and potential applications.

Acknowledgements

The authors would like to thank the Karlsruhe Nano Micro Facility (KNMF) for the access to the electron microscopy and spectroscopy unit.

Disclosure statement

No potential conflict of interest was reported by the authors.

Funding

The authors would like to thank the Helmholtz Association (Germany) for financial support through the Helmholtz Portfolio Project 'Electrochemical Storage in System—Reliability and Integration'. A. S. acknowledges support of DAAD–IIT Master-Sandwich programme 2015–2016.

References

[1] Rost CM, Sachet E, Borman T, et al. Entropy-stabilized oxides. Nat Commun. 2015;6:8485.
[2] Yeh J-W, Chen S-K, Lin S-J, et al. Nanostructured high-entropy alloys with multiple principal elements: novel alloy design concepts and outcomes. Adv Eng Mater. 2004;6:299–303.
[3] Zhang Y, Zuo TT, Tang Z, et al. Microstructures and properties of high-entropy alloys. Prog Mater Sci. 2014;61:1–93.
[4] Tsai M-H, Yeh J-W. High-entropy alloys: a critical review. Mater Res Lett. 2014;2:107–123.
[5] Murty BS, Yeh JW, Ranganathan S. High-entropy alloys. London: Butterworth-Heinemann; 2014.
[6] Hsieh M-H, Tsai M-H, Shen W-J, Yeh J-W. Structure and properties of two Al–Cr–Nb–Si–Ti high-entropy nitride coatings. Surf Coat Technol. 2013;221:118–123.
[7] Shen WJ, Tsai MH, Tsai KY, et al. Superior oxidation resistance of $(Al_{0.34}Cr_{0.22}Nb_{0.11}Si_{0.11}Ti_{0.22})$50N50 high-entropy nitride. J Electrochem Soc. 2013;160:C531–C535.
[8] Braic V, Vladescu A, Balaceanu M, Luculescu CR, Braic M. Nanostructured multi-element (TiZrNbHfTa)N and (TiZrNbHfTa)C hard coatings. Surf Coat Technol. 2012;211:117–121.
[9] Bérardan D, Franger S, Dragoe D, Meena AK, Dragoe N. Colossal dielectric constant in high entropy oxides. Phys Status Solidi-R. 2016;10:328–333.
[10] Djenadic R, Botros M, Benel C, et al. Nebulized spray pyrolysis of Al-doped $Li_7La_3Zr_2O_{12}$ solid electrolyte for battery applications. Solid State Ionics. 2014;263:49–56.
[11] Benel C, Darbandi AJ, Djenadic R, et al. Synthesis and characterization of nanoparticulate $La_{0.6}Sr_{0.4}CoO_3-\delta$ cathodes for thin-film solid oxide fuel cells. J Power Sources. 2013;229:258–264.
[12] Darbandi AJ, Enz T, Hahn H. Synthesis and characterization of nanoparticulate films for intermediate temperature solid oxide fuel cells. Solid State Ionics. 2009;180:424–430.

[13] Sieger H, Suffner J, Hahn H. Thermal stability of nanocrystalline Sm_2O_3 and Sm_2O_3–MgO. J Am Ceram Soc. 2006;89:979–984.
[14] Messing GL, Zhang S-C, Jayanthi GV. Ceramic powder synthesis by spray pyrolysis. J Am Ceram Soc. 1993;76:2707–2726.
[15] Murugavel P, Kalaiselvam M, Raju AR, Rao CNR. Submicrometre spherical particles of TiO_2, ZrO_2 and PZT by nebulized spray pyrolysis of metal–organic precursors. J Mater Chem. 1997;7:1433–1438.
[16] Rustad JR. Density functional calculations of the enthalpies of formation of rare-earth orthophosphates. Am Mineral. 2012;97:791–799.
[17] Adachi G, Imanaka N, Kang ZC. Binary rare earth oxides. Dordrecht: Kluwer Academic; 2005.
[18] Zinkevich M. Thermodynamics of rare earth sesquioxides. Prog Mater Sci. 2007;52:597–647.
[19] Greis O. A contribution to the structural chemistry of A-type rare earth sesquioxides. J Solid State Chem. 1980;34:39–44.
[20] Shannon RD. Revised effective ionic radii and systematic studies of interatomic distances in halides and chalcogenides. Acta Crystallogr. 1976;32:751–767.
[21] Djenadic R, Botros M, Hahn H. Is Li-doped $MgAl_2O_4$ a potential solid electrolyte for an all-spinel Li-ion battery? Solid State Ionics. 2016;287:71–76.
[22] Topas V5. General profile and structure analysis software for powder diffraction data. User's manual. Karlsruhe: Bruker AXS; 2015.
[23] Schneider CA, Rasband WS, Eliceiri KW. NIH Image to ImageJ: 25 years of image analysis. Nat Methods. 2012;9:671–675.
[24] Darbandi AJ. Nanoparticulate cathode films for low temperature solid oxide fuel cells [dissertation]. Darmstadt (Germany): Technische Universität Darmstadt; 2012.
[25] Bêche E, Charvin P, Perarnau D, Abanades S, Flamant G. Ce 3d XPS investigation of cerium oxides and mixed cerium oxide (CexTiyOz). Surf Interface Anal. 2008;40:264–267.
[26] Holleman AF, Wiberg EN. Lehrbuch der anorganischen chemie (textbook of inorganic chemistry). Berlin: Walter de Gruyter; 1995.
[27] Sawangphruk M, Foord JS. Localized electrodeposition of praseodymium oxide on boron-doped diamond. Diam Relat Mater. 2010;19:885–888.
[28] Ogasawara H, Kotani A, Potze R, Sawatzky GA, Thole BT. Praseodymium 3d- and 4d-core photoemission spectra of Pr_2O_3. Phys Rev B. 1991;44:5465–5469.
[29] Baronetti GT, Grosso WE, Maina SP, et al. Surface praseodymium species on MgO: characterization and activity for oxidative coupling of methane. J Chem Technol Biot. 1997;70:141–146.
[30] Pauling L. The principles determining the structure of complex ionic crystals. J Am Chem Soc. 1929;51:1010–1026.
[31] Troparevsky MC, Morris JR, Kent PRC, Lupini AR, Stocks GM. Criteria for predicting the formation of single-phase high-entropy alloys. Phys Rev X. 2015;5:011041.
[32] Abel J, Lamirand-Majimel M, Majimel J, et al. Oxygen non-stoichiometry phenomena in $Pr1-xZrxO_2-y$ compounds ($0.02 < x < 0.5$). Dalton T. 2014;43:15183–15191.
[33] Tabira Y, Withers RL, Minervini L, Grimes RW. Systematic structural change in selected rare earth oxide pyrochlores as determined by wide-angle CBED and a comparison with the results of atomistic computer simulation. J Solid State Chem. 2000;153:16–25.
[34] Tsai K-Y, Tsai M-H, Yeh J-W. Sluggish diffusion in Co–Cr–Fe–Mn–Ni high-entropy alloys. Acta Mater. 2013;61:4887–4897.